Chem Biol Drug Des 2012; **80:** 426–433

Research Article

doi: 10.1111/j.1747-0285.2012.01421.x

Discovery, Synthesis and Evaluation of Novel Cholesterol Absorption Inhibitors

Xiaoyun Zhu†, Jianfeng Ji†, Dandan Huang, Yan Zhu, Chunlei Tang, Xuan Yang, Hai Qian* and Wenlong Huang*

Centre of Drug Discovery, State Key Laboratory of Natural Medicines, China Pharmaceutical University, 24 Tongjiaxiang, Nanjing 210009, China
**Corresponding authors: Hai Qian, qianhai24@163.com; Wenlong Huang, ydhuangwenlong@126.com*
†These authors contributed equally to this work.

Chemical-based common feature pharmacophore modelling of Niemann Pick C1 Like 1 inhibitors was performed to provide some insights on the important pharmacophore features essential for Niemann Pick C1 Like 1 inhibition using Discovery Studio V2.5. After in-house database screening, a new series of substituted oxazolidinones, selected from the top ranked hits, have been synthesized and evaluated as novel cholesterol absorption inhibitors. All compounds demonstrated effect of different degrees in lowering the total cholesterol in serum, especially compounds 1a, 2a and 2d, the potency of which was comparable to that of ezetimibe. It was also found that 1a, 1d and 2d could raise high-density lipoprotein cholesterol levels markedly. Interestingly, compounds 2a–2f appeared to have the moderate potential to lower triglyceride levels, which were superior to that of normal cholesterol absorption inhibitors including ezetimibe.

Key words: cholesterol absorption inhibitor, Niemann Pick C1 Like 1, oxazolidinones, pharmacophore

Abbreviations: NPC1L1, Niemann Pick C1 Like 1; LDL, low-density lipoprotein; DS, Discovery Studio; TC, total cholesterol; HDL-C, high-density lipoprotein cholesterol; TG, triglyceride; HA, hydrogen bond acceptor; HD, hydrogen bond donor; HY, hydrophobic.

Received 20 February 2012, revised 18 April 2012 and accepted for publication 8 May 2012

High serum cholesterol levels have been unequivocally implicated as a cause of coronary artery disease, which is the major cause of death and cardiovascular morbidity in the world (1). Along with statins, which lower low-density lipoprotein (LDL) cholesterol levels by inhibition of cholesterol biosynthesis mediated by HMG-CoA reductase, the approval of the cholesterol absorption inhibitor, ezetimibe (Figure 1), has been shown to be effective in decreasing blood LDL cholesterol levels by decreasing uptake of dietary cholesterol (2,3). Clinically, as a monotherapy, ezetimibe achieves an average 18% reduction in LDL. When used in combination with a statin, ezetimibe affords an additional 15–18% reduction in LDL beyond that achieved by the statin alone (4). Ezetimibe was discovered using an empirical, *in vivo* screening protocol (3). However, researchers at Schering-Plough/Merck recently demonstrated that it inhibited cholesterol absorption via binding to Niemann Pick C1 Like 1 (NPC1L1) which was highly expressed in the proximal intestine and was a key mediator of cholesterol transport (5). Thus NPC1L1 lies in the ezetimibe sensitive pathway for cholesterol absorption, making it a likely candidate for the target of ezetimibe (6).

The substituted azetidinone (7), ezetimibe, is currently commercially available for the treatment of hypercholesterolemia. However, the effectiveness of available antilipidemic therapies is limited, in part because of poor patient compliance due to unacceptable side effects and tolerability as well as minimal efficacy or potency (8). Moreover, certain drug products may not be advantageous to all patients because of genetic polymorphisms regarding cholesterol biosynthesis. Furthermore, potential side effects of absorption of certain azetidinones may be detrimental. For these reasons, there is a continuing need for novel antilipidemic agents that may be used alone or in combination with other agents that provide increased efficacy and tolerability with decreased toxicity (9).

In the present investigation, we have generated *Common Feature Pharmacophore* models using Discovery Studio V2.5 (DS) for NPC1L1 inhibitors. Then the best pharmacophore model was used as a 3D query to screen in-house database for identifying new cholesterol absorption inhibitors. The hit compounds were subsequently subjected to filtering by Lipinski's rule of five. And several substituted oxazolidinones (Figure 1), selected from the top ranked hits, have been synthesized and evaluated as novel cholesterol absorption inhibitors.

Methods and Materials

Pharmacophore modelling studies

Pharmacophore model generation

A training set of 12 reported NPC1L1 inhibitors with binding affinity, as listed in Figure S1 in the Supporting Information (10,11), were used to generate the pharmacophore model after added hydrogen. Before starting the pharmacophore generation process, conformational analysis of the molecules was performed using the polling algorithm. The conformers of training set were generated using the *BEST* methods. The *Common Feature Pharmacophore Generation*

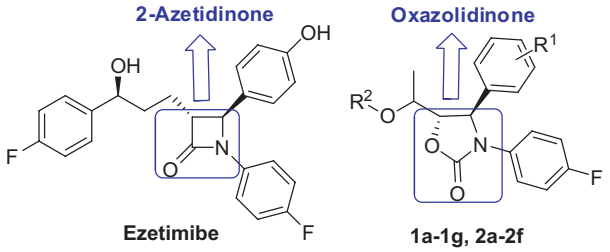

Figure 1: Structures of ezetimibe and target compounds **1a–1g**, **2a–2f**.

protocol implemented in DS V2.5 was applied to construct the model.

Database screening

The best pharmacophore model was used as a 3D structural query for retrieving potent molecules from in-house database comprised of 530 compounds which were designed as cholesterol absorption inhibitors. For each molecule in the database, 255 conformers were generated with the fast conformer generation method, allowing a maximum energy of 20 kcal/mol above that of the most stable conformation. The database screening was carried out using *ligand pharmacophore mapping* protocol implemented in DS with best/flexible search option (12). The hit compounds were subsequently subjected to filtering by Lipinski's rule of five. And two classes of substituted oxazolidinones (Figure 1), selected from the top ranked hits, were subjected to further studies.

Chemistry

All reagents were purchased from Shanghai Chemical Reagent Company (Shanghai, China). Column chromatography (CC): silica gel 60 (100–200 mesh). Thin-layer chromatography: silica gel 60 F254 plates (250 mm; Qingdao Ocean Chemical Company, Qingdao, China). M.p.: capillary tube; uncorrected. IR spectra: Shimadzu FTIR-8400S spectrophotometer; per cm. ^{1}H NMR spectra: Bruker ACF-300Q apparatus at 300 MHz, in $CDCl_3$ unless otherwise indicated; δ in ppm rel. to Me_4Si, J in Hz. Mass spectrometry (MS): Hewlett-Packard 1100 LC/MSD spectrometer, in m/z; Elemental analyses: CHN-O-Rapid instrument; %Purity of the target compounds (>97%) were determined by HPLC analysis (UV detector, wavelength: 230 nm, mobile phase composed of ammonium acetate buffer (0.02 M, pH adjusted to 7.0 with ammonium hydroxide) and acetonitrile).

General procedure for the preparation of 4

Hydroxyacetone (23.25 mmol), 4-fluoroaniline (15.5 mmol), **3** (14.1 mmol) and L-proline (2.82 mmol) were dissolved in DMSO (150 mL) under nitrogen and stirred for 12 h at room temperature. The reaction mixture was extracted with ammonium chloride solution (300 mL) and EtOAc (2 × 150 mL). The organic layers were washed with saturated sodium chloride solution and dried with Na_2SO_4, filtered and evaporated to dryness. The residue was then purified using column chromatography with a (PE/EtOAc 6:1, V/V) to afford **4**.

General procedure for the preparation of 5

Compound **4** (7.38 mmol) was dissolved in CH_2Cl_2 (50 mL) under nitrogen followed by the addition of triethylamine (14.76 mmol) and chilled to −20 °C. A solution of triphosgene (7.38 mmol) dissolved in CH_2Cl_2 (30 mL) was then added drop-wise over 15 min. The reaction mixture was stirred overnight allowing it to warm to 25 °C over this period. The reaction was quenched by the addition of a saturated solution of ammonium chloride (100 mL). The layers were separated, organic layer dried with Na_2SO_4, filtered and evaporated to dryness, yielding the brown oily residue which was purified by column chromatography (PE/EtOAc 8:1, V/V) to provide **5**.

General procedure for the preparation of 6

Compound **5** (13.2 mmol) was dissolved in anhydrous methanol (80 mL) and cooled to −10 °C. Sodium borohydride (6.6 mmol) was then added portion-wise to the reaction and the mixture allowed to warm to 25 °C, stirred for 3 h. A 2 M HCl was then added to the reaction and extracted with EtOAc, the resulting layers separated, organic layer dried with Na_2SO_4, filtered and evaporated to dryness. The resulting compound was purified using column chromatography (PE/EtOAc 5:1, V/V) to provide **6**.

General procedure for the preparation of 1d–1g, 2c–2f and 7–11

Compound **6** (3 mmol), corresponding acid (3 mmol) and 4-dimethylaminopyridine (DMAP) (0.2 equiv.) were dissolved anhydrous CH_2Cl_2 (80 mL), A solution of dicyclohexylcarbodiimide (DCC) (4.5 mmol) dissolved in CH_2Cl_2 (20 mL) was then added drop-wise over 10 min. The reaction mixture was stirred overnight at room temperature. The mixture allowed to cool to −5 °C, stand for 6 h. The reaction mixture filtered and evaporated to dryness. The resulting compound was purified using column chromatography (PE/EtOAc) to provide **1d–1g, 2c–2f** and **7–11**.

General procedure for the preparation of 1a–1c and 2a–2b

Compounds **7–11** (3 mmol) dissolved in a mixture of EtOAc (10 mL) and methanol (10 mL), and 10% Pd/C (10% weight) was then added to the reaction. The reaction mixture was stirred at room temperature for 8 h, filtered and evaporated to dryness. The resulting compound was purified using column chromatography (PE/EtOAc) to afford **1a–1c** and **2a–2b.**

1-((4R,5S)-3-(4-fluorophenyl)-4-(4-hydroxyphenyl)-2-oxooxazolidin-5-yl)ethyl 3-methylbenzoate (1a)

Yield: 79.6%. Yellow powder, m.p.: 110–111 °C. ^{1}H-NMR (300 MHz, $CDCl_3$) δ: 9.55–9.54 (s, 1H, -OH), 7.72–7.60 (m, 4H, Ar-H), 7.30–7.18 (m, 4H, Ar-H), 7.15–7.04 (m, 2H, Ar-H), 6.90–6.71 (m, 2H, Ar-H), 5.37–5.33 (m, 1H, -$OCHCH_3$), 5.10–5.08 (d, 1H, -CHN-, J = 4.5 Hz), 4.42–4.40 (m, 1H, -OCH-), 2.21 (s, 3H, -$ArCH_3$), 1.43–1.42 (m, 3H, -CH_3). IR (KBr, per cm) υ: 3411, 2925, 2855, 1724, 1615, 1511, 1451, 1427, 1275, 1106, 1050, 929, 834, 785, 682. MS (70eV) m/z: 436.3

([M + H]$^+$). Anal. calcd. for $C_{25}H_{22}FNO_5$: C, 68.96; H, 5.09; N, 3.22; Found (%): C, 68.86; H, 5.12; N, 3.21%.

1-((4R,5S)-3-(4-fluorophenyl)-4-(4-hydroxyphenyl)-2-oxooxazolidin-5-yl)ethyl benzo[d][1,3]dioxole-5-carboxylate (1b)

Yield: 78.8%. White powder, m.p.: 114–115 °C. ^{1}H-NMR (300 MHz, DMSO-d_6) δ: 9.55–9.54 (s, 1H, -OH), 7.56–7.42 (m, 4H, Ar-H), 7.29–7.10 (m, 5H, Ar-H), 6.90–6.71 (m, 2H, Ar-H), 6.11–6.10 (s, 2H, -OCH_2O-), 5.72–5.43 (d, 1H, -CHN-, J = 4.5 Hz), 5.35–5.32 (m, 1H, -$OCHCH_3$), 4.60–4.59 (m, 1H, -OCH-), 1.40–1.39 (m, 3H, -CH_3). IR (KBr, per cm) υ: 3412, 2986, 1731, 1615, 1512, 1489, 1444, 1383, 1277, 1159, 1037, 927, 834, 760, 647. MS (70 eV) m/z: 466.3 ([M + H]$^+$). Anal. calcd. for $C_{25}H_{20}FNO_7$: C, 64.51; H, 4.33; N, 3.01; Found: C, 64.60; H, 4.29; N, 2.98%.

1-((4R,5S)-3-(4-fluorophenyl)-4-(4-hydroxyphenyl)-2-oxooxazolidin-5-yl)ethyl 2-phenylacetate (1c)

Yield: 81.2%. Brown oil. ^{1}H-NMR (300 MHz, DMSO-d_6) δ: 9.57 (s, 1H, -OH), 7.53–7.26 (m, 6H, Ar-H), 7.15–7.05 (m, 5H, Ar-H), 6.93–6.88 (m, 2H, Ar-H), 5.40–5.28 (d, 1H, -CHN-, J = 5.1 Hz), 5.16–5.08 (m, 1H, -$OCHCH_3$), 4.48–4.04 (m, 1H, -OCH-), 3.56–3.34 (s, 2H, $ArCH_2CO$-), 1.28–1.26 (m, 3H, -CH_3). IR (KBr, per cm) υ: 3319, 2935, 1736, 1614, 1598, 1512, 1402, 1307, 1228, 1066, 835, 764, 696. MS (70 eV) m/z: 458.3 ([M + Na]$^+$). Anal. calcd. for $C_{25}H_{22}FNO_5$: C, 68.96; H, 5.09; N, 3.22; Found: C, 69.02; H, 5.07; N, 3.25%.

1-((4R,5S)-3-(4-fluorophenyl)-4-(4-methoxyphenyl)-2-oxooxazolidin-5-yl)ethyl 3-methylbenzoate (1d)

Yield: 75.4%. White powder, m.p.: 119–121 °C. ^{1}H-NMR (300 MHz, DMSO-d_6) δ: 7.51–7.40 (m, 4H, Ar-H), 7.39–7.28 (m, 6H, Ar-H), 7.18–6.90 (m, 2H, Ar-H), 5.85–5.57 (d, 1H, -CHN-, J = 4.2 Hz), 5.38–5.31 (m, 1H, -$OCHCH_3$), 4.65–4.61 (m, 1H, -CHO-), 3.72 (s, 3H, -OCH_3), 2.16 (s, 3H, -$ArCH_3$), 1.47–1.40 (m, 3H, -CH_3). IR (KBr, per cm) υ: 3651, 3414, 3072, 2960, 2935, 1754, 1716, 1588, 1513, 1460, 1352, 1231, 1131, 1045, 942, 847, 760, 683. MS (70 eV) m/z: 472.3 ([M + Na]$^+$). Anal. calcd. for $C_{26}H_{24}FNO_5$: C, 69.48; H, 5.38; N, 3.12; Found: C, 69.54; H, 5.39; N, 3.14%.

1-((4R,5S)-3-(4-fluorophenyl)-4-(4-methoxyphenyl)-2-oxooxazolidin-5-yl)ethyl 4-nitrobenzoate (1e)

Yield: 83.6%. White powder, m.p.: 120–122 °C. ^{1}H-NMR (300 MHz, DMSO-d_6) δ: 8.83–8.80 (m, 2H, Ar-H), 7.52–7.47 (m, 2H, Ar-H), 7.44–7.29 (m, 4H, Ar-H), 7.18–7.08 (m, 2H, Ar-H), 6.94–6.89 (m, 2H, Ar-H), 5.84–5.66 (d, 1H, -CHN-, J = 5.1 Hz), 5.48–5.45 (m, 1H, -OCH-CH_3), 4.74–4.71 (m, 1H, -OCH-), 3.70 (s, 3H, -OCH_3), 1.51–1.46 (m, 3H, -CH_3). IR (KBr, per cm) υ: 3483, 3075, 2936, 1759, 1612, 1586, 1513, 1442, 1428, 1306, 1193, 971, 824, 752, 624. MS (70 eV) m/z: 503.2 ([M + Na]$^+$). Anal. calcd. for $C_{25}H_{21}FN_2O_7$: C, 62.50; H, 4.41; N, 5.83; Found: C, 62.56; H, 4.39; N, 5.86%.

1-((4R,5S)-4-(2,3-dimethoxyphenyl)-3-(4-fluorophenyl)-2-oxooxazolidin-5-yl)ethyl 3-methylbenzoate (1f)

Yield: 84.5%. Colourless oil. ^{1}H-NMR (300 MHz, DMSO-d_6) δ: 7.69–7.42 (m, 4H, Ar-H) 7.37–7.21 (m, 4H, Ar-H), 6.91–6.88 (m, 3H, Ar-H), 5.88–5.60 (d, 1H, -CHN-, J = 3.3 Hz), 5.39–5.32 (m, 1H, -$OCHCH_3$), 4.68–4.67 (m, 1H, -OCH-), 4.06 (s, 3H, -OCH_3), 3.91 (s, 3H, -OCH_3), 2.13 (s, 3H, -$ArCH_3$), 1.46–1.44 (m, 3H, -CH_3). IR (KBr, per cm) υ: 3319, 2938, 1758, 1721, 1590, 1512, 1484, 1397, 1275, 1132, 1069, 834, 764. MS (70 eV) m/z: 480.4 ([M + H]$^+$). Anal. calcd. for $C_{27}H_{26}FNO_6$: C, 67.63; H, 5.47; N, 2.92; Found: C, 67.68; H, 5.36; N,2.90%.

1-((4R,5S)-4-(2,3-dimethoxyphenyl)-3-(4-fluorophenyl)-2-oxooxazolidin-5-yl)ethyl 4-nitrobenzoate (1g)

Yield: 83.0%. Yellow powder, m.p.: 157–159 °C. ^{1}H-NMR (300 MHz, DMSO-d_6) δ: 8.84–8.81 (m, 2H, Ar-H), 7.69–7.32 (m, 4H, Ar-H), 7.29–7.01 (m, 2H, Ar-H), 6.73–6.70 (m, 3H, Ar-H), 5.88–5.72 (d, 1H, -CHN-, J = 4.2 Hz), 5.53–5.47(m, 1H, -$OCHCH_3$), 4.76–4.73 (m, 1H, -OCH-), 4.04 (s, 3H, -OCH_3), 3.95 (s, 3H, -OCH_3), 1.51–1.49 (m, 3H, -CH_3). IR (KBr, per cm) υ: 3462, 3101, 2935, 1760, 1628, 1589, 1547, 1512, 1484, 1462, 1397, 1345, 1167, 1070, 921, 833, 772. MS (70 eV) m/z: 533.2 ([M + Na]$^+$). Anal. calcd. for $C_{26}H_{23}FN_2O_8$: C, 61.17; H, 4.54; N, 5.49; Found: C, 61.21; H, 4.55; N, 5.53%.

1-((4R,5S)-3-(4-fluorophenyl)-4-(4-hydroxyphenyl)-2-oxooxazolidin-5-yl)ethyl 2-phenoxyacetate (2a)

Yield: 73.8%. Yellow powder, m.p.: 77–78 °C. ^{1}H-NMR (300 MHz, $CDCl_3$) δ: 7.30–7.19 (m, 4H, Ar-H), 7.14–6.91 (m, 4H, Ar-H), 6.89–6.77 (m, 5H, Ar-H), 5.38–5.30 (m, 1H, -$OCHCH_3$), 4.99–4.98 (d, 1H, -CHN-, J = 5.4 Hz), 4.73 (s, 2H, -OCH_2CO-), 4.40–4.38 (m, 1H, -OCH-), 1.44–1.35 (M, 3H, -CH_3). IR (KBr, per cm) υ: 3407, 2985, 2937, 1751, 1615, 1599, 1511, 1449, 1224, 1052, 868, 785, 690. MS (70 eV) m/z: 474.2 ([M + Na]$^+$). Anal. calcd. for $C_{25}H_{22}FNO_6$: C, 66.51; H, 4.91; N, 3.10; Found: C, 66.55; H, 4.87; N, 3.13%.

1-((4R,5S)-3-(4-fluorophenyl)-4-(4-hydroxyphenyl)-2-oxooxazolidin-5-yl)ethyl 2-methyl-2-phenoxypropanoate (2b)

Yield: 74.9%. Yellow oil. ^{1}H-NMR (300 MHz, DMSO-d_6) δ: 9.75 (s, 1H, -OH), 7.43–7.31 (m, 4H, Ar-H), 7.30–7.06 (m, 4H, Ar-H), 7.02–6.70 (m, 5H, Ar-H), 5.41–5.23 (d, 1H, -CHN-, J = 4.5 Hz), 5.24–5.18 (m, 1H, -$OCHCH_3$), 4.53–4.48 (m, 1H, -OCH-), 1.45 (s, 6H, -$C(CH_3)_2$), 1.29–1.25 (m, 3H, -CH_3). IR (KBr, per cm) υ: 3330, 2990, 2925, 1836, 1615, 1597, 1512, 1453, 1385, 1275, 1173, 1054, 972, 834, 753, 696. MS (70 eV) m/z: 502.2 ([M + Na]$^+$). Anal. calcd. for $C_{27}H_{26}FNO_6$: C, 67.63; H, 5.47; N, 2.92; Found: C, 67.71; H, 5.45; N, 2.95%.

1-((4R,5S)-3-(4-fluorophenyl)-4-(4-methoxyphenyl)-2-oxooxazolidin-5-yl)ethyl 2-phenoxyacetate (2c)

Yield: 68.7%. Yellow oil. ^{1}H-NMR (300 MHz, DMSO-d_6) δ: 7.30–7.10 (m, 6H, Ar-H), 6.98–6.96 (m, 2H, Ar-H), 6.92–6.86 (m, 5H, Ar-H),

5.50–5.38 (d, 1H, -CHN-, J = 5.1 Hz), 5.26–5.18 (m, 1H, -$OCHCH_3$), 4.87–4.69 (s, 2H, -OCH_2CO-), 4.55–4.49 (m, 1H, -OCH-), 3.71 (s, 3H, -OCH_3), 1.33–1.31 (m, 3H, -CH_3). IR (KBr, per cm) υ: 3319, 2988, 1758, 1560, 1512, 1495, 1397, 1275, 1193, 1089, 835, 692. MS (70 eV) m/z: 488.2 ([M + Na]$^+$). Anal. calcd. for $C_{26}H_{24}FNO_6$: C, 67.09; H, 5.20; N, 3.01; Found: C, 67.14; H, 5.18; N, 2.99%.

1-((4R,5S)-3-(4-fluorophenyl)-4-(4-methoxyphenyl)-2-oxooxazolidin-5-yl)ethyl 2-(4-chlorophenoxy)acetate (2d)

Yield: 73.9%. Yellow oil. ^{1}H-NMR (300 MHz, DMSO-d_6) δ: 7.49–7.40 (m, 2H, Ar-H), 7.39–7.28 (m, 4H, Ar-H), 7.15–7.10 (m, 2H, Ar-H), 6.93–6.90 (m, 4H, Ar-H), 5.48–5.37 (d, 1H, -CHN-, J = 5.4 Hz), 5.25–5.18 (m, 1H, -$OCHCH_3$), 4.87–4.73 (s, 2H, -OCH_2CO-), 4.53–4.48 (m, 1H, -OCH-), 3.71 (s, 3H, -OCH_3), 1.31–1.30 (m, 3H, -CH_3). IR (KBr, per cm) υ: 3472, 1753, 1618, 1513, 1491, 1384, 1192, 824, 641. MS (70 eV) m/z: 522.2 ([M + Na]$^+$). Anal. calcd. for $C_{26}H_{23}ClFNO_6$: C, 62.47; H, 4.64; Cl, 7.09; N, 2.80; Found: C, 62.38; H, 4.65; N, 2.81%.

1-((4R,5S)-4-(2,3-dimethoxyphenyl)-3-(4-fluorophenyl)-2-oxooxazolidin-5-yl)ethyl 2-phenoxyacetate (2e)

Yield: 77.6%. Yellow oil. ^{1}H-NMR (300 MHz, $CDCl_3$) δ: 7.40–7.21 (m, 5H, Ar-H), 7.05–6.76 (m, 7H, Ar-H), 5.44–5.32(d, 1H, -CHN-, J = 4.2 Hz), 5.42–5.30 (m, 1H, -$OCHCH_3$), 4.62 (s, 2H, -OCH_2CO-), 4.44–4.31(m, H, -OCH-), 3.90 (s, 3H,-OCH_3), 3.81 (s, 3H,-OCH_3), 1.46–1.39 (m, 3H, -CH_3). IR (KBr, per cm) υ: 3319, 2936, 1758, 1599, 1512, 1485, 1398, 1273, 1192, 835, 756, 691. MS (70 eV) m/z: 496.3 ([M + H]$^+$). Anal. calcd. for $C_{27}H_{26}FNO_7$: C, 65.45; H, 5.29; N, 2.83; Found: C, 65.47; H, 5.31; N, 2.79%.

1-((4R,5S)-4-(2,3-dimethoxyphenyl)-3-(4-fluorophenyl)-2-oxooxazolidin-5-yl)ethyl 2-methyl-2-phenoxypropanoate (2f)

Yield: 73.4%. Colourless oil. ^{1}H-NMR (300 MHz, DMSO-d_6) δ: 7.47–7.23 (m, 5H, Ar-H), 7.07–6.80 (m, 5H, Ar-H), 5.52–5.51 (d, 1H, -CHN-, J = 4.2 Hz), 5.24–5.21 (m, 1H, -$OCHCH_3$), 4.57–4.56 (m, 1H, -OCH-), 3.81 (s, 3H, -OCH_3), 3.71 (s, 3H, -OCH_3), 1.46 (s, 6H, -$C(CH_3)_2$), 1.26–1.23 (m, 3H, -CH_3). IR (KBr, per cm) υ: 3319, 2988, 1758, 1596, 1512, 1486, 1397, 1275, 1133, 1070, 834, 695. MS (70 eV) m/z: 524.3 ([M + H]$^+$). Anal. calcd. for $C_{29}H_{30}FNO_7$: C, 66.53; H, 5.78; N, 2.68; Found: C, 66.46; H, 5.79; N, 2.70%.

Evaluation of hypocholesterolemic effects

Cholesterol absorption inhibitory activities of new substituted oxazolidinones **1a–1g** and **2a–2f** were assessed in orally dosed, cholesterol-fed Sprague-Dawley rats as reported in literature (7,13). Hypocholesterolemic Sprague-Dawley rats were used to test the efficacy of these compounds. Male Sprague-Dawley rats, weighing between 200 and 250 g, were maintained on rodent chow and provided with water. In order to induce a hypercholesterolemia in Sprague-Dawley rats, their chow diet must be supplemented with 1% cholesterol and 0.5% cholic acid. Treatment protocols consisted of feeding this diet for 7 days. Test compounds, dissolved in 0.5 mL corn oil, were administered to the animals by oral gavage daily (mid-light cycle) during this time period. On the last day, the animals were sacrificed and blood sample was taken for lipid analyses. Plasma cholesterol levels, triglyceride (TG) levels and high-density lipoprotein cholesterol (HDL-C) levels were determined by a commercial modification of the cholesterol oxidase method which was available in a kit form.

Results and Discussion

Pharmacophore modelling studies

By analysis of the chemical nature of the training set compounds, important feature types, such as hydrogen bond acceptor (HA), hydrogen bond donor (HD) and hydrophobic (HY), were selected for each pharmacophore model generation. Finally, several pharmacophore models were generated, of which the best model contains one HD, two HAs and two HY features (Figure 2). The common features model was used as a 3D query to screen in-house database, as a result, 73 compounds were hit, then filtering by Lipinski's rule of five. Two classes of representative oxazolidinones (13 compounds) were selected, and subjected to synthesis and evaluation (Table 1).

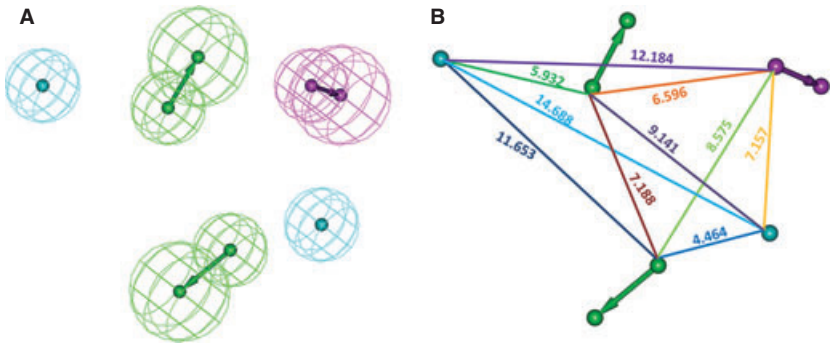

Figure 2: The best pharmacophore model for Niemann Pick C1 Like 1(NPC1L1) inhibitors where HA, HD and HY are illustrated in green, magenta and cyan, respectively. (A) The best pharmacophore model for NPC1L1 inhibitors. (B) 3D spatial relationship and distance constraints of the model. HA, hydrogen bond acceptor; HD, hydrogen bond donor; HY, hydrophobic.

Table 1: Structures of the synthesized oxazolidinones

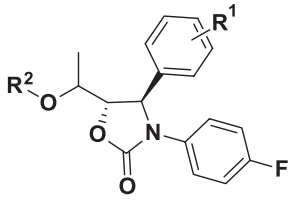

Compound	R^1	R^2	Compound	R^1	R^2
1a	4-OH	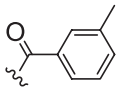	**2a**	4-OH	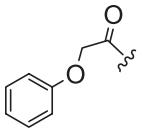
1b	4-OH	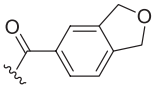	**2b**	4-OH	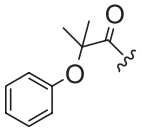
1c	4-OH	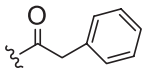	**2c**	4-OCH_3	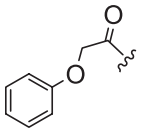
1d	4-OCH_3	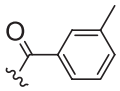	**2d**	4-OCH_3	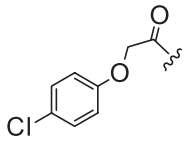
1e	4-OCH_3	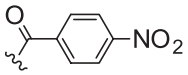	**2e**	2,3-OCH_3	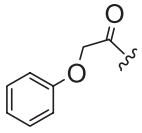
1f	2,3-OCH_3	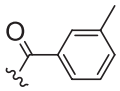	**2f**	2,3-OCH_3	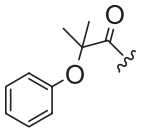
1g	2,3-OCH_3	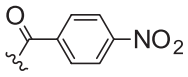			

Chemistry

The structures of the substituted oxazolidinones **1a–1g** and **2a–2f** are presented in Table 1. All the compounds were characterized by spectroscopic methods. These compounds were prepared according to the sequence of reactions, illustrated in Scheme 1. Utilizing an asymmetric three-component Mannich reaction reported by List and coworkers (10,11), hydroxyacetone (**1**) was subsequently reacted with 4-fluoroaniline (**2**), substituted benzaldehyde **3** in the presence of catalytic L-proline to afford 1,2-amino alcohol **4** in moderate yield and excellent stereoselectivity. Treatment of **4** with triphosgene and triethylamine resulted in the formation of oxazolidinone **5**. Reducing reaction of the side chain ketone provided alcohol **6** by treatment with $NaBH_4$ in ethanol/ethyl acetate. Compounds **7–11**, **1d–1g** and **2c–2f** were prepared by coupling alcohol **6** to corresponding acid in the presence of DCC/DMAP, and **7–11** were subsequently debenzylated using transfer hydrogenation conditions to afford corresponding oxazolidinones **1a–1c** and **2a–2b**.

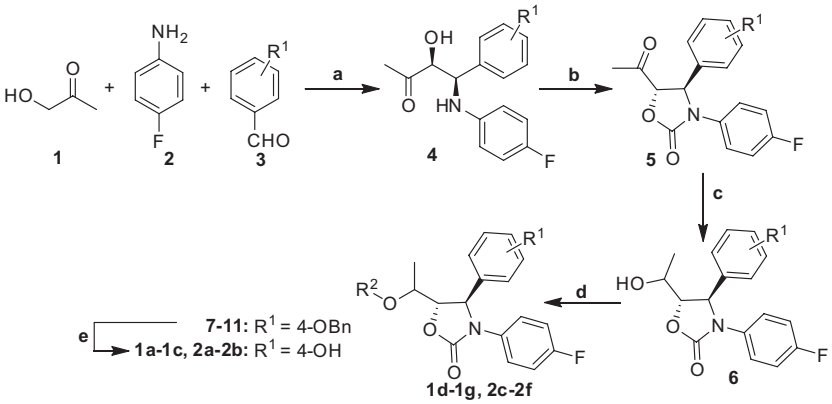

Reagents and conditions: (a) L-proline (20 mol%), DMSO, 25ºC, 12 h; (b) triphosgene, Et_3N, CH_2Cl_2, –20ºC~25ºC, 12 h; (c) $NaBH_4$, CH_3OH, –10ºC~25ºC; (d) DMAP/DCC, CH_2Cl_2, r.t.; (e) H_2, Pd/C (10%), EtOH/EtOAc, r.t. .

Scheme 1: Synthesis of the target compounds **1a–1g** and **2a–2f** [Reagents and conditions: (a) L-proline (20 mol%), DMSO, 25 °C, 12 h; (b) triphosgene, Et_3N, CH_2Cl_2, –20 °C–25 °C, 12 h; (c) $NaBH_4$, CH_3OH, –10 °C–25 °C; (d) 4-dimethylaminopyridine (DMAP)/dicyclohexylcarbodiimide (DCC), CH_2Cl_2, r.t.; (e) H_2, Pd/C (10%), EtOH/EtOAc, r.t.].

In vivo cholesterol absorption inhibitory activities

Cholesterol absorption inhibition was assessed in orally dosed, cholesterol-fed Sprafue-Dawley rats as previously described (13). The results were presented in Table 2. As can be seen from the data, all of the new compounds demonstrated effect of different degrees in lowering the total cholesterol (TC) in serum, especially compounds **1a**, **2a** and **2d**, the potency of which was comparable to that of ezetimibe. It was also found that **1a**, **1d** and **2d** could raise HDL-C levels markedly. More interestingly, compounds **2a–2f** appeared to have the moderate potential to lower the TG levels, which was superior to that of normal cholesterol absorption inhibitors including ezetimibe. The possible reason for this interesting phenomenon is that the synthesized compounds **2a–2f** were designed by the introduction of derivatives of the phenoxyacetic scaffold of clofibrate into side chain of oxazolidinones (Figure 3). The fibric-acid derivatives–bezafibrate, ciprofibrate, clofibrate, fenofibrate and gemfibrozil–primarily decrease TG by increasing lipoprotein lipase activity and by decreasing the release of free fatty acids from peripheral adipose tissue (14).

Table 2 shows the Best Fit values of the selected compounds together with their corresponding experimental TC values. The best pharmacophore model, which aligned to ezetimibe and compound **1a** that was the most potent derivative of this series as representative examples, is shown in Figure 4. As can be seen from Figure 4, the result suggests that the best pharmacophore model perfectly fits ezetimibe. From the overall analysis, we conclude that the best pharmacophore model truly reflects the features of NPC1L1 inhibitors.

Table 2: Cholesterol absorption inhibition and mapping results of new synthesized oxazolidinones and reference compound

Compound[a]	TC[b] (% reduction)	TG[c] (% reduction)	HDL-C[d] (% increase)	Best Fit value[e]
1a	49.91**	NE	29.69**	4.57
1b	11.98	NE	5.12	3.56
1c	36.71*	NE	19.05	4.35
1d	22.69	NE	34.31**	4.29
1e	16.34	NE	25.25	3.43
1f	30.38	NE	12.64	3.92
1g	16.61	NE	21.03	3.75
2a	48.72**	5.67	23.86*	4.4
2b	14.73	10.19	22.05	3.89
2c	29.01	5.06	25.37*	3.68
2d	42.26**	12.23*	27.13**	4.09
2e	28.88*	6.04	14.32	3.43
2f	27.04	8.46	10.37	3.54
Ezetimibe	48.3**	NE	37.66**	4.41

HDL-C, high-density lipoprotein cholesterol; TC, total cholesterol; TG, triglyceride; NE, no effect.

**$p < 0.01$; *$p < 0.05$ as compared with the high-cholesterol diets group.

[a]6–8 Sprague-Dawley rats per group; dose: 50 mg/kg.

[b]Reduction of total cholesterol comparing to the one in animals fed by high-cholesterol diets.

[c]Reduction of triglyceride comparing to the one in animals fed by high-cholesterol diets.

[d]Increase of HDL-C comparing to the one in animals fed by high-cholesterol diets.

[e]Best Fit value indicates how well the features in the pharmacophore overlap the chemical features in the molecule.

Conclusions and Future Directions

In this study, chemical based common feature pharmacophore modelling of NPC1L1 inhibitors has been created using DS. The common feature pharmacophore model was performed to provide some insights on the important pharmacophore features essential for NPC1L1 inhibition. After in-house database screening, a new series of substituted oxazolidinones, selected from the top ranked hits, have been synthesized and evaluated as novel cholesterol absorption inhibitors. Among all of these derivatives, compounds **1a**, **2a** and **2d** demonstrated high potencies to lower the TC in serum, the potencies of which were comparable to that of the reference compound, ezetimibe. Moreover, compounds **1a**, **1d** and **2d** could raise HDL-C levels markedly. Compounds **2a–2f** appeared interestingly to

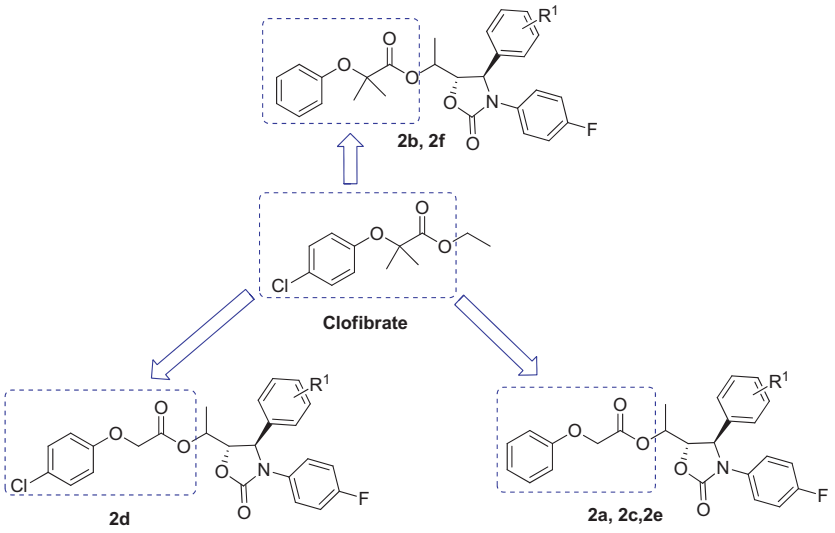

Figure 3: Structures of clofibrate and target compounds **2a–2f**. Synthesized compounds **2a–2f** were designed by introduction of derivatives of the phenoxyacetic scaffold of clofibrate into side chain of oxazolidinones.

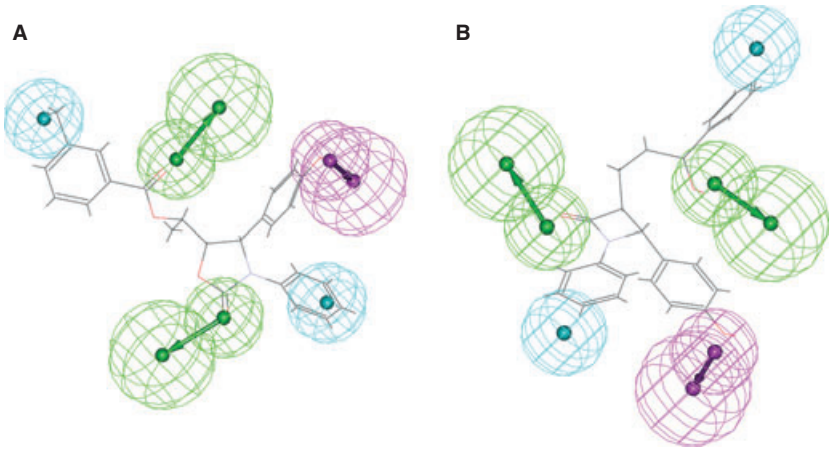

Figure 4: The best pharmacophore model aligned to ezetimibe and compound **1a**. (A) The best model aligned to compound **1a**. (B) The best model aligned to ezetimibe. HA, HD and HY are illustrated in green, magenta and cyan, respectively. HA, hydrogen bond acceptor; HD, hydrogen bond donor; HY, hydrophobic.

have the moderate potential to lower TG levels. Compound **2d** with phenoxyacetic side chain showed the better potencies in raising HDL-C levels, lowering TC levels, lowering TG levels and pharmacophore feature mapping (Best Fit value: 4.09), respectively. It may be considered as a promising candidate for the development of potent agents for treatment of coronary artery disease.

Acknowledgments

This study was supported by the National Natural Science Foundation of China (No. 81172932); the Project Program of State Key Laboratory of Natural Medicines, China Pharmaceutical University (No. JKGZ201103); and the Fundamental Research Funds for the Central Universities of China (No. 2J10023 and JKY2011009).

References

1. Iyer S.P., Yao X., Crona J.H., Hoos L.M., Tetzloff G., Davis H.R. Jr, Graziano M.P., Altmann S.W. (2005) Characterization of the putative native and recombinant rat sterol transporter Niemann-Pick C1 Like 1 (NPC1L1) protein. Biochim Biophys Acta;1722: 282–292.
2. Clader J.W. (2004) The discovery of ezetimibe: a view from outside the receptor. J Med Chem;47:1–9.
3. McMasters D.R., Garcia-Calvo M., Maiorov V., McCann M.E., Meurer R.D., Bull H.G., Lisnock J., Howell K.L., Devita R.J. (2009) Spiroimidazolidinone NPC1L1 inhibitors. 1: discovery by 3D-similarity-based virtual screening. Bioorg Med Chem Lett;19:2965–2968.
4. Burnett J.R., Huff M.W. (2006) Cholesterol absorption inhibitors as a therapeutic option for hypercholesterolaemia. Expert Opin Investig Drugs;15:1337–1351.
5. Burnett D.A. (2004) Beta-lactam cholesterol absorption inhibitors. Curr Med Chem;11:1873–1887.
6. Wang Y., Qian H., Huang W., Zhang H., Zhou J. (2011) Synthesis and biological evaluation of ezetimibe analogs as possible cholesterol absorption inhibitors. Lett Drug Des Discov;8:500–505.
7. Wang Y., Zhang H., Huang W., Kong J., Zhou J., Zhang B. (2009) 2-Azetidinone derivatives: design, synthesis and evaluation of cholesterol absorption inhibitors. Eur J Med Chem;44:1638–1643.

8. Sampalis J.S., Bissonnette S., Boukas S. (2011) Effectiveness of ezetimibe in reducing the estimated risk for fatal cardiovascular events in hypercholesterolaemic patients with inadequate lipid control while on statin monotherapy as measured by the SCORE model. Adv Prev Med;2011:1–7.
9. Kashani A., Sallam T., Bheemreddy S., Mann D.L., Wang Y., Foody J.M. (2008) Review of side-effect profile of combination ezetimibe and statin therapy in randomized clinical trials. Am J Cardiol;101:1606–1613.
10. Pfefferkorn J.A., Larsen S.D., Van Huis C., Sorenson R., Barton T., Winters T., Auerbach B. *et al.* (2008) Substituted oxazolidinones as novel NPC1L1 ligands for the inhibition of cholesterol absorption. Bioorg Med Chem Lett;18:546–553.
11. Ritter T., Kvaerno L., Werder M., Hauser H., Carreira E.M. (2005) Heterocyclic ring scaffolds as small-molecule cholesterol absorption inhibitors. Org Biomol Chem;3:3514–3523.
12. Zhu X., Huang D., Lan X., Tang C., Zhu Y., Han J., Huang W., Qian H. (2011) The first pharmacophore model for potent G protein-coupled receptor 119 agonist. Eur J Med Chem;46:2901–2907.
13. Salisbury B.G., Davis H.R., Burrier R.E., Burnett D.A., Bowkow G., Caplen M.A., Clemmons A.L. *et al.* (1995) Hypocholesterolemic activity of a novel inhibitor of cholesterol absorption, SCH 48461. Atherosclerosis;115:45–63.
14. Farmer J.A., Gotto A.M. Jr (1995) Currently available hypolipidaemic drugs and future therapeutic developments. Baillieres Clin Endocrinol Metab;9:825–847.

Supporting Information

Additional Supporting Information may be found in the online version of this article:

Figure S1. Structures and NPC1L1 binding affinity of training set.

Please note: Wiley-Blackwell is not responsible for the content or functionality of any supporting materials supplied by the authors. Any queries (other than missing material) should be directed to the corresponding author for the article.